



## Heteroaromatization with 4-phenyldiazenyl-1-naphthol. Part III: One-pot synthesis and DFT study of 4H-naphthopyran derivatives

Hany Mostafa Mohamed<sup>1,2</sup>, Ashraf Hassan Fekry Abd El-Wahab<sup>1,2,\*</sup> and Tarek Maamon El-Gogary<sup>1,3</sup>

<sup>1</sup>Chemistry Department, Faculty of Science, Jazan University, 2097, Jazan, Kingdom Saudi Arabia

<sup>2</sup>Chemistry Department, Faculty of Science, Al-Azhar University, 11884, Nasr City, Cairo, Egypt

<sup>3</sup>Chemistry Department, Faculty of Science (Domyat), Damietta University, 34517, Domyat Al-Gideda, Egypt

\*Corresponding author at: Chemistry Department, Faculty of Science, Jazan University, 2097, Jazan, Kingdom Saudi Arabia.

Tel.: +966.054.0963753. Fax: +966.017.3230028. E-mail address: [ash\\_abdelwahab@yahoo.com](mailto:ash_abdelwahab@yahoo.com) (A.H.F.A. El-Wahab).

### ARTICLE INFORMATION



DOI: 10.5155/eurjchem.8.4.358-366.1632

Received: 21 July 2017

Received in revised form: 23 August 2017

Accepted: 04 September 2017

Published online: 31 December 2017

Printed: 31 December 2017

### KEYWORDS

Malononitrile  
Fukui functions  
Ethyl cyanoacetate  
4-Phenyldiazenyl-1-naphthol  
4H-Naphthopyran derivatives  
Density Functional Theory (DFT)

### ABSTRACT

A one pot three component reaction of 4-phenyldiazenyl-1-naphthol (1), *p*-chloro benzaldehyde (2) and malononitrile or ethyl cyanoacetate (3) in ethanol/piperidine under reflux afforded 2-amino-4-(*p*-chlorophenyl)-6-phenyldiazenyl-4H-naphtho[1,2-*b*]pyrano-3-carbonitrile (4a) and ethyl 2-amino-4-(*p*-chlorophenyl)-6-phenyldiazenyl-4H-naphtho[1,2-*b*]pyrano-3-carboxylate (4b). Structure of these compounds was established on the basis of IR, <sup>1</sup>H NMR, <sup>13</sup>C NMR, Mass and UV-Vis spectra. Molecular geometry of compounds 4a and b was obtained at B3LYP/6-31+G(d) level. Two tautomers and two conformers were geometrically optimized. The tautomers are separated by about 7.942 kcal/mol while rotational conformers are only separated by 0.511 kcal/mol. Molecular reactivity descriptors including global electrophilicity, hardness, softness and local condensed Fukui functions were computed and discussed. Frontier molecular orbitals (HOMO and LUMO) were also computed.

Cite this: *Eur. J. Chem.* 2017, 8(4), 358-366

### 1. Introduction

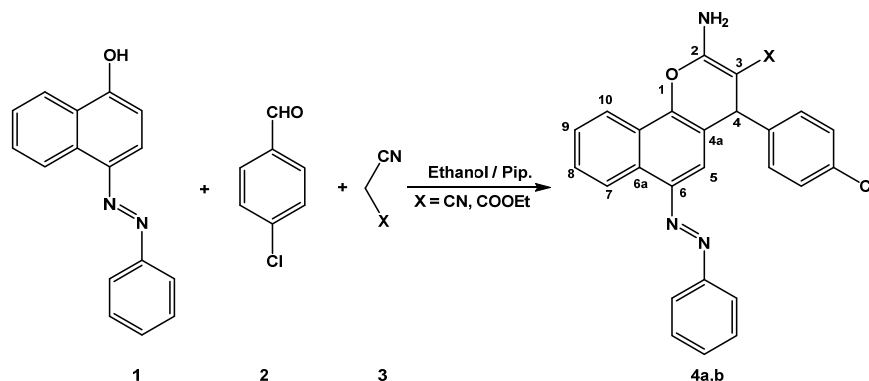
Synthetic azo compounds are widely used in different application fields, such as medicines, cosmetics, food, paints, plastics, shipbuilding, automobile industry and cable manufacture [1-12]. Moreover, azo compounds are known for their antineoplastics [13], antidiabetics [14], antiseptics [15], antibacterial [16] and antitumor activities [17]. 4H-Pyran nucleus is a fertile source of biologically important molecules possessing a wide spectrum of biological and pharmacological activities such as antimicrobial [18-21], inhibitors of influenza virus sialidases [22,23], DNA strand-breaking activity and mutagenicity [24], antiviral agent [25], antiproliferation agent [26], sex pheromone [27], antitumor [28,29] and central nervous system (CNS) activity [18-30]. The synthesis of 4H-naphthopyrans involves a one-pot three-component coupling reaction of, *p*-chlorobenzaldehyde, malononitrile or ethyl cyanoacetate and phenyldiazenyl-1-naphthol. Nowadays, multi-component reactions (MCRs) provide significant advantages over normal linear step synthesis, in terms of easy work-up procedures and purification, short reaction time, energy and raw-material consumption. The present work reports the results of molecular geometrical data for compound 2-amino-

4-(*p*-chlorophenyl)-6-(phenyldiazenyl)-4H-naphtho[1,2-*b*]pyran-3-carbonitrile (4a) and ethyl 2-amino-4-(*p*-chlorophenyl)-6-(phenyldiazenyl)-4H-naphtho[1, 2-*b*]pyran-3-carboxylate (4b) were computed using quantum density functional theory at B3LYP/6-31G(d) and chemical reactivity descriptors were computed to explore the reactivity of compound 4a and 4b.

### 2. Experimental

#### 2.1. Instrumentation

Melting points were determined with a Stuart Scientific Co., Ltd. apparatus. UV spectra were measured on a Shimadzu UV-1601PC UV-Vis spectrophotometer. IR spectra were determined as KBr pellets on a Jasco FT/IR 460 plus spectrophotometer. <sup>1</sup>H NMR and <sup>13</sup>C NMR spectra were recorded using a Bruker AV 400 MHz spectrometer. Mass spectra were measured on a Shimadzu GC/MS-QP5050A spectrometer. Elemental analyses were performed on a Perkin-Elmer 240 microanalyser in the Faculty of Science, Cairo University, Egypt.



Scheme 1

## 2.2. Synthesis of 4H-naphthopyran derivatives (4a and b)

To a mixture of 4-phenyldiazenyl-1-naphthol (2.48 g, 10 mmol), *p*-chlorobenzaldehyde (1.40 g, 10 mmol) and malononitrile (0.66 g, 10 mmol) or ethylcyano acetate (1.13 g, 10 mmol) in absolute ethanol (30 mL) was added a catalytic amount of piperidine (0.5 mL). The reaction mixture was heated until complete precipitation occurred (Reaction times: 2 h for compound **4a**; 5 h for compound **4b**) (Scheme 1). The solid product formed which was collected by filtration and recrystallized from dioxane and ethanol/benzene mixture, respectively.

**2-Amino-4-(*p*-chlorophenyl)-6-(phenyl diazenyl)-4H-naphtho[1,2-*b*]pyran-3-carbonitrile (4a):** Color: Yellow crystals. Yield: 90 %. M.p.: 245-246 °C. FT-IR (KBr,  $\nu$ ,  $\text{cm}^{-1}$ ): 3417, 3327, 3207 (NH<sub>2</sub>), 3001, 2960, 2812 (CH str.), 2196 (CN), 1666 (C=C), 1510 (N=N). <sup>1</sup>H NMR (400 MHz, CDCl<sub>3</sub>,  $\delta$ , ppm): 8.93-7.24 (m, 14H, Ar-H), 4.95 (s, 1H, CH-Pyran), 4.84 (bs, 2H, NH<sub>2</sub>, exchangeable by D<sub>2</sub>O). <sup>13</sup>C NMR (100 MHz, CDCl<sub>3</sub>,  $\delta$ , ppm): 158.59 (C-2), 152.94 (C-6), 144.70, 142.63, 133.44, 131.41, 133.29, 129.45, 129.20, 129.14, 127.82, 127.43, 123.75, 123.71, 123.28, 123.17, 120.90 (Ar-C), 116.98 (CN), 61.33 (C-3), 40.74 (C-4). MS (EI,  $m/z$  (%)): 438 (M<sup>+</sup>+2, 0.1), 436 (M<sup>+</sup>, 20.4), 325 (75.8), 220 (59.9), 77 (100), 51 (18.2). UV/Vis (CH<sub>3</sub>COCH<sub>3</sub>,  $\lambda_{\text{max}}$ , nm): 268.80. Anal. calcd for C<sub>26</sub>H<sub>17</sub>ClN<sub>4</sub>O: C, 71.48; H, 3.92; N, 12.82. Found: C, 71.01; H, 3.40; N, 12.39%.

**Ethyl 2-amino-4-(*p*-chlorophenyl)-6-(phenyl diazenyl)-4H-naphtho[1,2-*b*]pyran-3-carboxylate (4b):** Color: Yellow crystals. Yield: 75 %. M.p.: 208-209 °C. FT-IR (KBr,  $\nu$ ,  $\text{cm}^{-1}$ ): 3417, 3380, 3126 (NH<sub>2</sub>), 3060, 3010, 2960, (CH str.), 1675 (CO), 1629 (C=C), 1539 (N=N). <sup>1</sup>H NMR (400 MHz, CDCl<sub>3</sub>,  $\delta$ , ppm): 8.92-7.20 (m, 14H, Ar-H), 6.54 (bs, 2H, NH<sub>2</sub>, exchangeable by D<sub>2</sub>O), 5.14 (s, 1H, CH-Pyran), 4.11 (q, 2H,  $J = 7.0$  Hz, CH<sub>2</sub>), 1.21 (t, 3H,  $J = 7.0$  Hz, CH<sub>3</sub>). <sup>13</sup>C NMR (100 MHz, CDCl<sub>3</sub>,  $\delta$ , ppm): 169.15 (CO), 159.62 (C-2), 153.08 (C-6), 145.81, 145.79, 145.68, 144.26, 132.05, 131.24, 131.02, 129.61, 129.37, 129.13, 128.45, 128.36, 127.32, 127.00, 126.40, 123.79, 123.61, 123.11, 120.54, 112.76 (Ar-C), 79.01 (C-3), 59.73 (CH<sub>2</sub>), 40.37 (C-4), 14.37 (CH<sub>3</sub>). MS (EI,  $m/z$  (%)): 485 (M<sup>+</sup>+2, 5.41), 483 (M<sup>+</sup>, 9.22), 372 (35.2), 268 (18.5), 181 (6.7), 91 (100), 75 (60.1), 51 (9.3). UV/Vis (CH<sub>3</sub>COCH<sub>3</sub>,  $\lambda_{\text{max}}$ , nm): 267.58. Anal. calcd. for C<sub>28</sub>H<sub>22</sub>ClN<sub>3</sub>O<sub>3</sub>: C, 69.49; H, 4.58; N, 8.68. Found: C, 69.05; H, 4.12; N, 8.25%.

## 2.3. Computational details

All computations were done using Gaussian09 suite of programs [31]. Molecular geometry of anthraquinone compounds were optimized in the gas phase at DFT, B3LYP/6-31+G(d,p) level of theory. A frequency job was performed on the optimized geometry to confirm a minimum energy

structure. Fukui functions were calculated using DMol module [32,33] employing B3LYP/DND method implemented in Material Studio program [34].

## 3. Results and discussion

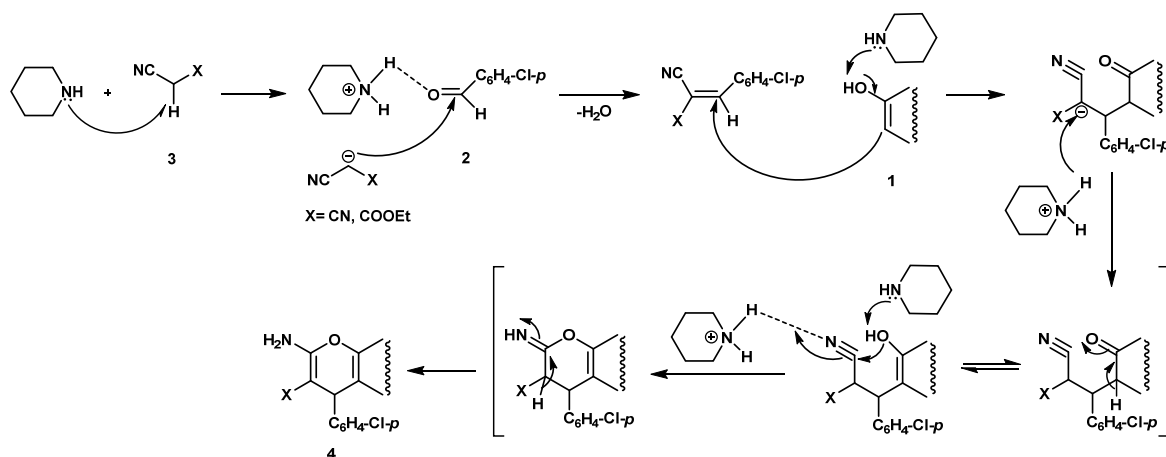
### 3.1. Synthesis

In continuation of previous work for synthesis of naphthopyrans with arylidene skeleton [20,21,35-40], we report herein the synthesis of naphthopyrans through three component condensation of aromatic aldehydes, malononitrile or ethyl cyanoacetate and naphthol. Thus, treatment of 4-phenyldiazenyl-1-naphthol (**1**), *p*-chlorobenzaldehyde (**2**) and malononitrile or ethyl cyanoacetate (**3**) in ethanol/piperidine under reflux afforded 2-amino-4-(*p*-chlorophenyl)-6-phenyldiazenyl-4H-naphtho[1,2-*b*]pyran-3-carbonitrile (**4a**) and ethyl 2-amino-4-(*p*-chlorophenyl)-6-phenyldiazenyl-4H-naphtho[1,2-*b*]pyran-3-carboxylate (**4b**), respectively (Scheme 1). Structure of these compounds was established on the basis of IR, UV, <sup>1</sup>H NMR, <sup>13</sup>C NMR and MS data.

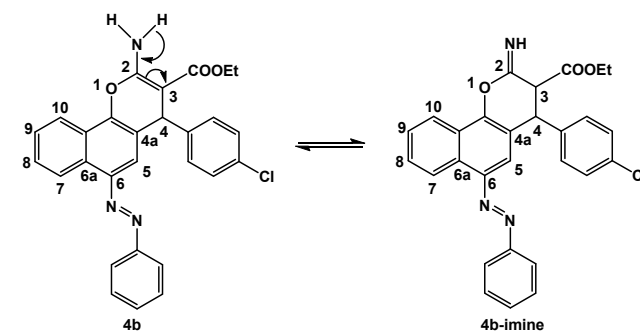
A plausible mechanism for the formation of naphthopyran derivatives catalyzed by piperidine is shown in Scheme 2. The Knoevenagel reaction in the presence of piperidine occurs via an initial formation of 2-(4-chlorobenzylidene)malononitrile or ethyl-3-(4-chlorophenyl)-2-cyanoacrylate, after removal of one molecule of water from the condensation of *p*-chlorobenzaldehyde and malononitrile or ethyl cyanoacetate. 4-Phenyldiazenyl-1-naphthol is converted to the enolate form after tautomerisation and attacks the of 2-(4-chlorobenzylidene)malononitrile or ethyl-3-(4-chlorophenyl)-2-cyanoacrylate as Michael acceptor, to give intermediate and then furnished the intermediate product, which upon intramolecular cyclization and rearrangement gave rise to 4H-naphthopyrans **4a** and **4b** (Scheme 2).

Structure of compound **4a** and **4b** was established on the basis of spectral data. The IR spectrum of compound **4a** showed the presence of a NH bands at  $\nu$  3417, 3327, 3207  $\text{cm}^{-1}$  and a CN band at  $\nu$  2196  $\text{cm}^{-1}$ , while for compound **4b** showed the appearance of a NH<sub>2</sub> bands  $\nu$  3417, 3380, 3126 and a CO band at  $\nu$  1675  $\text{cm}^{-1}$ . The UV spectra revealed a weak shoulder characteristic for 4H-pyran [41] at  $\lambda_{\text{max}}$  (CH<sub>3</sub>COCH<sub>3</sub>) 268.80-267.58 nm ( $\log \epsilon$  4.82-4.81).

By applying DFT, we shed light on the geometries and electronic properties. The compound which we have studied compound **4b** have two possibilities, two tautomer amino form and imino form; it was esteemed that imino form would be good as biologically active molecule. Then, we have compared the properties with compound **4b**. Moreover, the effect of NH<sub>2</sub> and NH at position 2 in compound **4b** and **4b**-imine (Scheme 3) has been studied.



Scheme 2



Scheme 3

The mass spectra of compounds **4a** and **4b** showed, the corresponding molecular ion peaks at  $m/z$  436 ( $M^+$ , 20.4) and 483 ( $M^+$ , 9.22). The  $^1\text{H}$  NMR and  $^{13}\text{C}$  NMR spectra of compound **4a** showed signals at  $\delta$  4.84 ppm for  $\text{NH}_2$  proton exchangeable by  $\text{D}_2\text{O}$ , at  $\delta$  4.95 ppm for  $\text{CH}$ -pyran proton and at  $\delta$  40.74 ppm for  $\text{CH}$ -pyran (C-4) carbon. In compound **4b**, the amino group gave 1H signals at  $\delta$  6.54 ppm for  $\text{NH}_2$  proton exchangeable by  $\text{D}_2\text{O}$ , at  $\delta$  5.14 ppm for  $\text{CH}$ -pyran proton and ester group at  $\delta$  4.11 ppm for  $\text{CH}_2$ , at  $\delta$  1.21 ppm for  $\text{CH}_3$ , with the corresponding signals in the  $^{13}\text{C}$  NMR at  $\delta$  169.15 ppm for carbonyl, at  $\delta$  59.73 ppm for  $\text{CH}_2$ , at  $\delta$  40.37 ppm for  $\text{CH}$ -pyran (C-4) and at  $\delta$  14.37 ppm  $\text{CH}_3$  carbon (Figure 1).

### 3.2. Molecular geometry

Molecular geometrical data for compound **4a** and **4b** were computed using quantum density functional theory DFT, at B3LYP/6-31G(d). Selected geometrical parameters are displayed in Figure 2. Both compounds **4a** and **4b** could be present in two tautomeric forms, amine and imine as shown in Figure 3. Each imine form could also be present in two conformations as shown in Figure 3. All these possible structures were studied and optimized at B3LYP/6-31G(d). Relative total energies are displayed in Figure 3. For compound **4a**, the amine tautomer is more stable than the imine one by about 6.866 kcal/mol while compound **4b** amine tautomer is more stable than the imine one by about 8.507 kcal/mol. The difference in relative energies between compound **4a** and **4b** is due to extra stabilization in compound **4b** via intramolecular hydrogen bonding as shown in Figure 3. Hydrogen bond distance  $\text{N}\cdots\text{O}$  is 1.977 Å in compound **4b** which is elongated to 2.077 Å in compound **4b**-imine-1. For compound **4a**, the

order of stability goes **4a** > **4a**-imine-2 > **4a**-imine-1. Imine conformers are inter-convertible at room temperature (difference is only 0.584 kcal/mol). For compound **4b**, the order of stability goes **4b** > **4b**-imine-2 > **4b**-imine-1. Imine conformers are also inter-convertible at room temperature (difference is only 0.438 kcal/mol).

The geometry of compound **4a** and **4b** were optimized at B3LYP/6-31+G(d). Based on tautomerization and conformational preferences three minimum energy structures were found as displayed in Figure 3. The computed geometrical parameters (Figure 2) show that the naphthalene ring and the two phenyl rings are perfect planar structures as shown from the dihedral angles ( $\sim 0.0^\circ$ ). The pyran ring is not that perfect planar where ring dihedral angles are between  $0.0$  and  $20.0^\circ$ . The *p*-chlorophenyl ring tends to perpendicular to the pyran ring with a torsion angle  $\sim 60.0^\circ$  in all structures. The amine structure in compound **4b** is stabilized by a weak intramolecular hydrogen bond  $\text{NH}\cdots\text{O}$  of length 1.977 Å and angle  $\text{N15-H43-O17}$   $126.7^\circ$ . Aromatic rings show typical values for  $\text{C-C}_{\text{ar}}$  ( $\sim 1.4$  Å) bond length and  $\text{C-C-C}$  bond angles ( $120^\circ$ ). The azo  $\text{N=N}$  distance is 1.260 Å in both structures.

### 3.3. Chemical reactivity

Chemical reactivity descriptors were computed to explore the reactivity of compound **4a** and **4b**. The density of electrons on an atom is an important property that contains all the information about the molecular systems. Descriptors of chemical reactivity are good tools for predicting and understanding reactivity of compounds. These descriptors initially developed within the density functional theory framework.

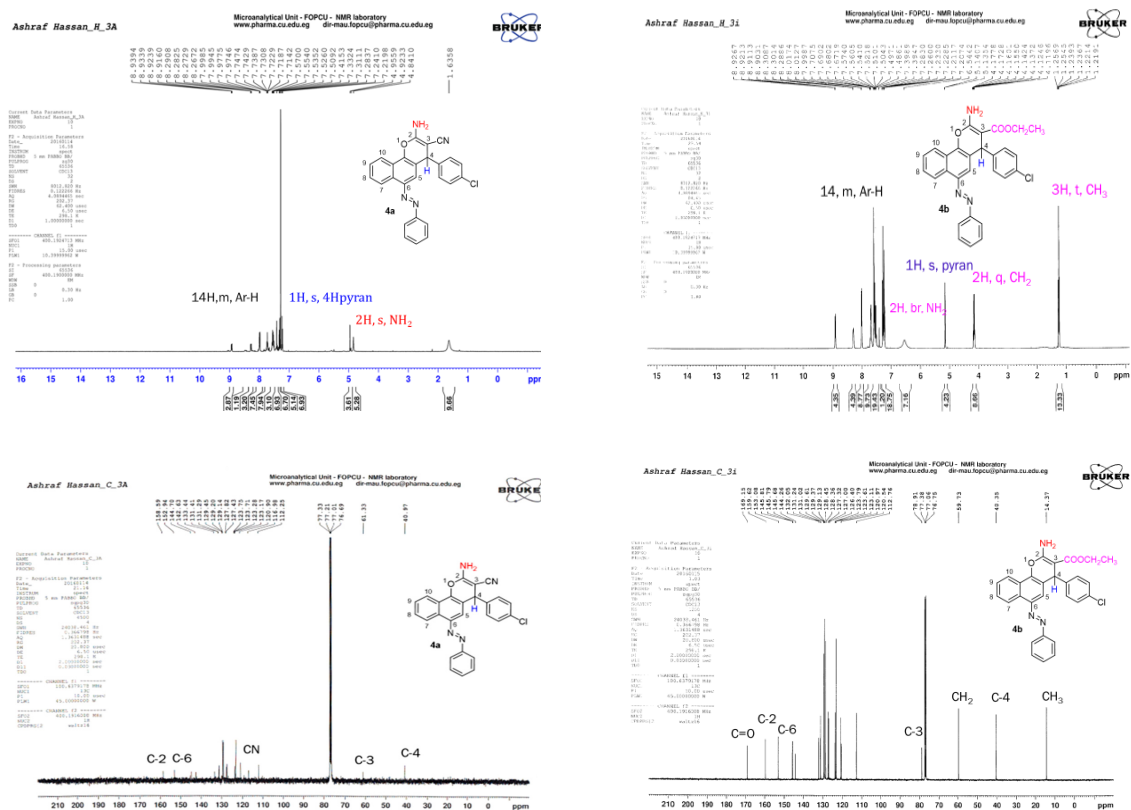


Figure 1.  $^1\text{H}$  NMR and  $^{13}\text{C}$  NMR spectral of compound **4a** and **4b**.

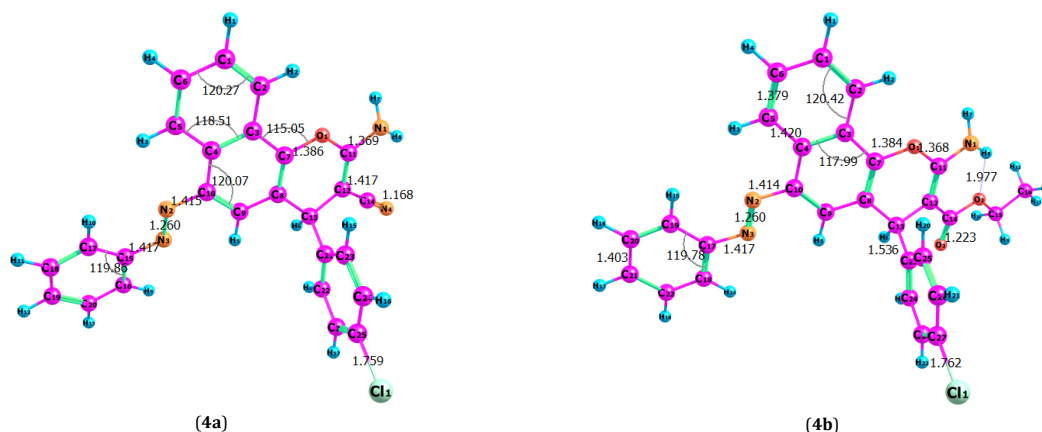


Figure 2. Optimized geometry of compound **4a** and **4b** at B3LYP/6-31+G(d) level.

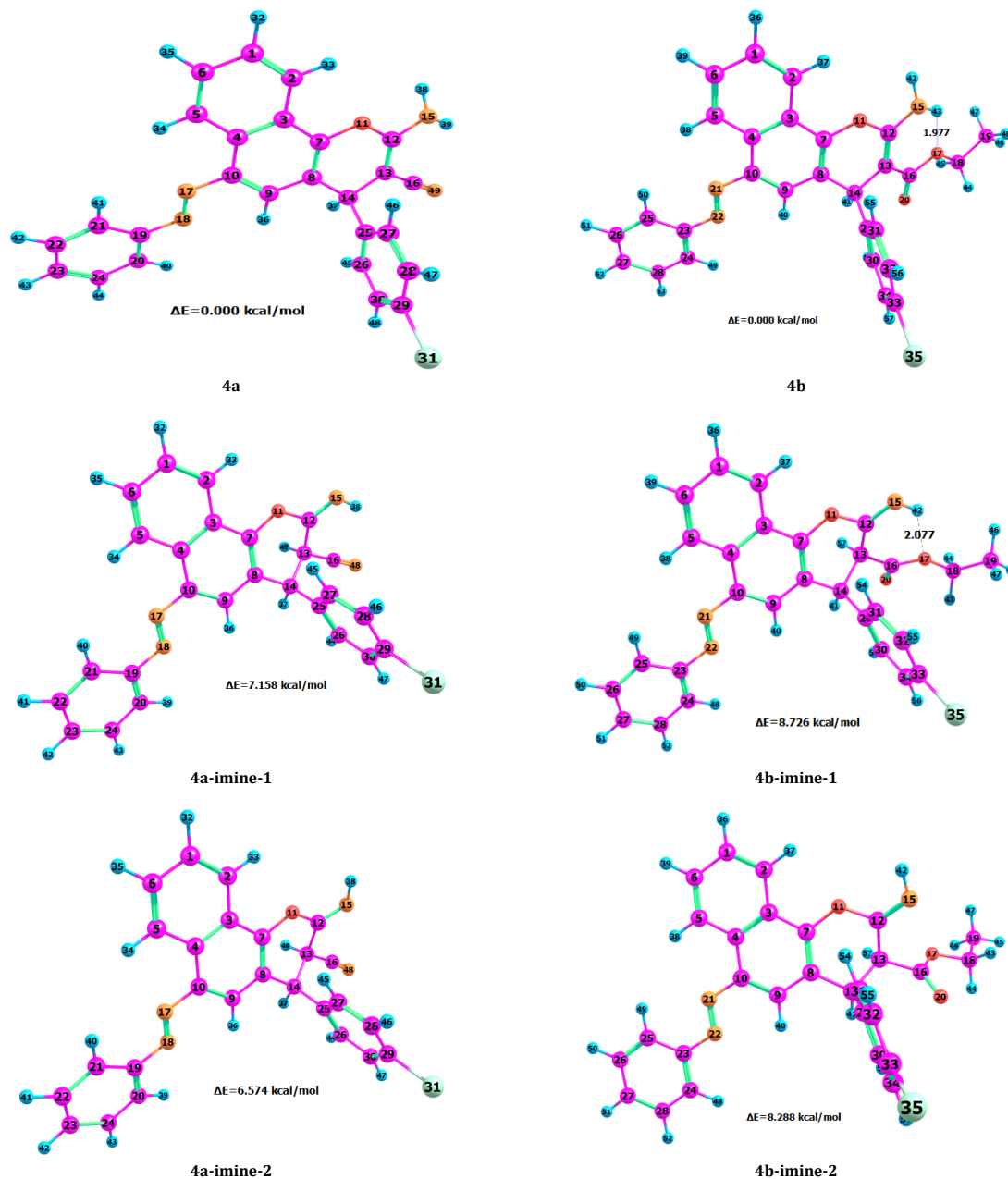
Global quantities as chemical potential ( $\mu$ ), electro-negativity ( $\chi$ ), chemical hardness ( $\eta$ ), chemical softness ( $S$ ), and electrophilicity ( $\omega$ ) of compounds **4a** and **4b** were calculated according to the equations presented elsewhere [42] and presented in Table 1. Softness of a molecule is a measure of its polarizability and hence, its reactivity. From the results in Table 1, it may be observed that the global softness of compound **4b** is larger than that of compound **4a**. Compound **4b** has the higher global electrophilicity (6.152) and higher softness (0.310). Chemical hardness ( $\eta$ ), reflects the resistance of the molecule to polarizability and hence susceptibility for chemical reaction. Chemical hardness ( $\eta$ ) for

compound **4b** (1.614) is smaller than that of compound **4a** (1.622).

Fukui [43] introduced a qualitative approach of chemical reactivity in the form of what we call Frontier Orbital Theory. Later, this theory was demonstrated [44,45] in the framework of DFT. In a molecular system, the atomic site, which possesses highest condensed Fukui function, favors the higher reactivity. Table 2 and 3 show the condensed Fukui functions as calculated based on Mulliken and Hirshfeld charges for compound **4a** and **4b**. Isosurface maps for Fukui functions of electrophilic, nucleophilic and radical attack for compound **4b** are given in Figure 4.

**Table 1.** Calculated global quantities: chemical potential ( $\mu$ ), electronegativity ( $\chi$ ), hardness ( $\eta$ ), softness ( $S$ ), and electrophilicity ( $\omega$ ) and energy of HOMO and LUMO and their difference.

Compound	$\mu$	$\chi$	$\eta$	$S$	$\omega$	$E_{\text{HOMO}}$	$E_{\text{LUMO}}$	$\Delta E_{\text{L-H}}$
4a	-4.467	4.467	1.622	0.308	6.152	-6.089	-2.845	3.244
4b	-4.289	4.289	1.614	0.310	5.700	-5.903	-2.675	3.227

**Figure 3.** Optimized structures of compound **4a** and **4b** and their tautomers and conformers showing their relative energies and H-bonding.

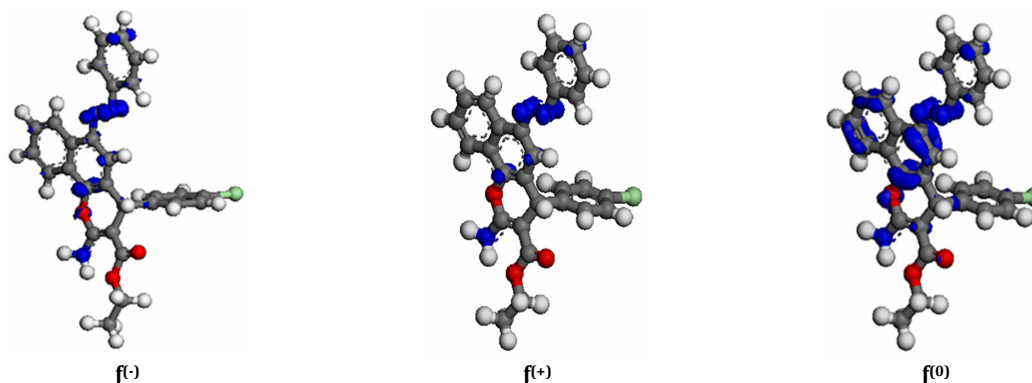
Isosurface maps show that compound **4b** acts better as nucleophile/electrophile than being involved in free radical attack. Naphthalene ring system, azo group, O-pyran and amino group in compound **4b** have the electrophilic/nucleophilic centers. On the other hand, free radical attack is shown on the azo group.

From the results of **Table 2** for compound **4a**, according to Hirshfeld charges the reactivity for the radical attack was found on  $\text{N}(18) > \text{C}(7) > \text{N}(49) > \text{N}(17) > \text{C}(23) > \text{C}9 > \text{C}6 > \text{C}1 > \text{C}2$ . For electrophilic attack, the most reactive sites are N18

(0.099) and N17 (0.092). The order of reactivity toward electrophilic attack could be ranked as  $\text{N}18 > \text{N}17 > \text{C}23 > \text{C}7 > \text{C}9 > \text{N}49 > \text{C}20 > \text{C}21$ . On the other hand, for nucleophilic attack, the most reactive site is N49 (0.061). The reactivity order toward nucleophilic attack could be ranked as  $\text{N}49 > \text{C}10 > \text{C}23 = \text{C}7 > \text{C}1 = \text{C}2 = \text{C}6 > \text{C}5 = \text{N}18$ . From **Table 3**, it is clear that compound **4b** is more reactive than compound **4a** when comparing values (Mulliken and Hirshfeld) of condensed Fukui functions for electrophilic attack as shown, also, from **Figure 4**.

**Table 2.** Condensed Fukui functions ( $f_k^0$ ) ( $f_k^+$ ) and ( $f_k^-$ ) indices of compound **4a**.

Atom	Radical attack		Electrophilic attack		Nucleophilic attack	
	Mulliken	Hirshfeld	Mulliken	Hirshfeld	Mulliken	Hirshfeld
C (1)	0.017	0.035	0.014	0.031	0.021	0.039
C (2)	0.025	0.033	0.020	0.026	0.030	0.039
C (3)	0.002	0.010	-0.002	0.012	0.005	0.009
C (4)	0.009	0.008	0.017	0.010	0.001	0.007
C (5)	0.016	0.024	0.003	0.009	0.030	0.038
C (6)	0.019	0.036	0.018	0.033	0.020	0.039
C (7)	0.060	0.049	0.071	0.053	0.049	0.045
C (8)	0.008	0.024	-0.005	0.017	0.022	0.031
C (9)	0.042	0.042	0.059	0.050	0.026	0.034
C (10)	0.027	0.032	0.001	0.015	0.052	0.050
O (11)	0.021	0.026	0.008	0.015	0.033	0.037
C (12)	-0.002	0.007	-0.004	0.004	0.000	0.010
C (13)	0.028	0.019	0.015	0.007	0.042	0.031
C (14)	-0.009	0.004	-0.004	0.002	-0.014	0.006
N (15)	0.014	0.016	0.012	0.014	0.016	0.018
C (16)	0.004	0.009	-0.001	0.005	0.008	0.013
N (17)	0.050	0.052	0.090	0.092	0.011	0.013
N (18)	0.066	0.069	0.098	0.099	0.033	0.038
C (19)	-0.003	0.012	-0.010	0.011	0.005	0.014
C (20)	0.024	0.031	0.027	0.035	0.021	0.026
C (21)	0.027	0.027	0.037	0.034	0.017	0.020
C (22)	0.005	0.026	0.003	0.030	0.006	0.022
C (23)	0.037	0.052	0.044	0.059	0.030	0.045
C (24)	0.007	0.027	0.008	0.032	0.006	0.023
C (25)	-0.012	-0.009	-0.013	-0.010	-0.011	-0.008
C (26)	-0.002	0.002	-0.003	0.000	-0.001	0.003
C (27)	-0.006	-0.004	-0.007	-0.004	-0.006	-0.004
C (28)	0.005	0.008	0.004	0.007	0.005	0.009
C (29)	0.001	0.010	0.000	0.009	0.001	0.012
C (30)	0.003	0.009	0.002	0.007	0.005	0.011
Cl (31)	0.037	0.030	0.034	0.027	0.041	0.033
H (32)	0.041	0.022	0.039	0.020	0.044	0.024
H (33)	0.033	0.018	0.032	0.017	0.034	0.019
H (34)	0.021	0.012	0.012	0.007	0.030	0.017
H (35)	0.040	0.021	0.036	0.020	0.043	0.023
H (36)	0.032	0.019	0.031	0.021	0.033	0.017
H (37)	0.021	0.011	0.012	0.006	0.029	0.016
H (38)	0.012	0.009	0.01	0.008	0.014	0.011
H (39)	0.015	0.011	0.014	0.01	0.017	0.012
H (40)	0.031	0.016	0.037	0.019	0.024	0.013
H (41)	0.022	0.013	0.028	0.017	0.015	0.009
H (42)	0.038	0.019	0.044	0.022	0.032	0.016
H (43)	0.044	0.026	0.050	0.030	0.039	0.022
H (44)	0.039	0.020	0.045	0.023	0.033	0.017
H (45)	0.008	0.003	0.006	0.002	0.010	0.004
H (46)	-0.005	-0.002	-0.004	-0.002	-0.006	-0.002
H (47)	0.016	0.008	0.014	0.007	0.017	0.008
H (48)	0.018	0.009	0.016	0.007	0.020	0.010
N (49)	0.055	0.049	0.044	0.037	0.067	0.061

**Figure 4.** Isosurface maps for Fukui functions of electrophilic, nucleophilic and radical attack for compound **4b**.

For nucleophilic attack, the highest Fukui function value is accommodated on the azo nitrogen N22 (0.098) and N21 (0.092). The order of the nucleophilic attack is N22 > N21 > C27 > C7 > C9 > C24. For electrophilic attack, the most nucleophilic site is C10 (Fukui function value is 0.054) and the tendency for electrophilic attack decreases as C10 > C7 > C27 >

C2 > C1=C5=C6 > N22. Compound **4b** has larger tendency for nucleophilic attack (0.098 on N22) than compound **4a** (0.061 on N49). Compound **4a** has larger tendency for electrophilic attack (0.099 on azo nitrogen) than compound **4b** (0.054 on C10).

**Table 3.** Condensed Fukui functions ( $f_k^0$ ) ( $f_k^+$ ) and ( $f_k^-$ ) indices of compound **4b**.

Atom	Radical attack		Electrophilic attack		Nucleophilic attack	
	Mulliken	Hirshfeld	Mulliken	Hirshfeld	Mulliken	Hirshfeld
C (1)	0.017	0.036	0.021	0.041	0.013	0.030
C (2)	0.026	0.034	0.033	0.043	0.020	0.026
C (3)	0.001	0.011	0.004	0.009	-0.002	0.012
C (4)	0.009	0.008	0.001	0.007	0.017	0.010
C (5)	0.017	0.025	0.032	0.041	0.002	0.009
C (6)	0.019	0.037	0.021	0.041	0.018	0.033
C (7)	0.063	0.051	0.055	0.049	0.072	0.053
C (8)	0.009	0.025	0.023	0.034	-0.006	0.017
C (9)	0.043	0.043	0.026	0.034	0.060	0.051
C (10)	0.027	0.034	0.055	0.054	0.000	0.014
O (11)	0.020	0.025	0.032	0.034	0.009	0.015
C (12)	0.004	0.004	0.004	0.005	-0.004	0.003
C (13)	0.024	0.015	0.035	0.025	0.013	0.006
C (14)	0.009	0.003	0.014	0.006	-0.005	0.001
N (15)	0.013	0.015	0.014	0.016	0.012	0.014
C (16)	0.011	0.009	0.012	0.010	0.01	0.007
O (17)	0.002	0.006	0.003	0.007	0.001	0.004
C (18)	0.009	0.004	0.011	0.004	-0.008	0.003
C (19)	0.004	0.003	0.005	0.004	-0.004	0.003
O (20)	0.021	0.019	0.027	0.024	0.015	0.014
N (21)	0.049	0.051	0.007	0.009	0.090	0.092
N (22)	0.065	0.068	0.033	0.039	0.097	0.098
C (23)	0.002	0.013	0.005	0.014	-0.009	0.011
C (24)	0.024	0.031	0.022	0.027	0.027	0.035
C (25)	0.027	0.028	0.018	0.021	0.037	0.034
C (26)	0.005	0.026	0.006	0.022	0.003	0.029
C (27)	0.038	0.052	0.031	0.046	0.044	0.059
C (28)	0.007	0.028	0.006	0.023	0.008	0.032
C (29)	0.010	0.009	0.009	0.008	-0.011	-0.01
C (30)	0.001	0.002	0.000	0.003	-0.003	0.001
C (31)	0.006	0.005	0.005	0.005	-0.006	-0.005
C (32)	0.004	0.007	0.005	0.008	0.004	0.006
C (33)	0.001	0.010	0.001	0.011	0.000	0.009
C (34)	0.004	0.010	0.005	0.011	0.003	0.008
Cl (35)	0.036	0.029	0.040	0.032	0.033	0.026
H (36)	0.042	0.022	0.046	0.024	0.039	0.020
H (37)	0.035	0.019	0.037	0.020	0.032	0.017
H (38)	0.021	0.012	0.032	0.017	0.011	0.007
H (39)	0.040	0.022	0.045	0.024	0.036	0.020
H (40)	0.033	0.02	0.035	0.018	0.032	0.021
H (41)	0.017	0.009	0.025	0.013	0.01	0.004
H (42)	0.010	0.008	0.011	0.009	0.009	0.007
H (43)	0.014	0.010	0.016	0.010	0.013	0.009
H (44)	0.010	0.005	0.011	0.005	0.008	0.004
H (45)	0.009	0.004	0.011	0.005	0.007	0.003
H (46)	0.015	0.008	0.017	0.009	0.013	0.007
H (47)	0.004	0.002	0.004	0.003	0.003	0.002
H (48)	0.005	0.003	0.005	0.003	0.004	0.002
H (49)	0.031	0.016	0.025	0.013	0.037	0.019
H (50)	0.021	0.013	0.015	0.009	0.028	0.017
H (51)	0.038	0.019	0.033	0.017	0.044	0.022
H (52)	0.044	0.026	0.039	0.022	0.050	0.030
H (53)	0.039	0.02	0.034	0.017	0.045	0.023
H (54)	0.008	0.003	0.010	0.004	0.007	0.002
H (55)	0.009	0.003	0.010	0.003	-0.008	-0.003
H (56)	0.015	0.007	0.016	0.008	0.014	0.006
H (57)	0.018	0.009	0.020	0.010	0.016	0.008

### 3.4. Frontier orbital analysis

Highest occupied molecular orbital (HOMO) and lowest unoccupied molecular orbital (LUMO) for compound **4a** and **4b** are calculated and presented in Figure 5. HOMO and LUMO, as frontier molecular orbitals, are considered as very important molecular parameters for the stability and chemical reactivity of the species [46,47]. HOMO and LUMO energies, and LUMO-HOMO energy gap ( $\Delta E_{L-H}$ ), in eV, are displayed in Table 1. The lower HOMO energy, the easier of that orbital to participate in chemical reaction by donating electrons. LUMO energy, on the other hand, determine the ability to accept an electron in a chemical change. LUMO-HOMO energy gap reflects the chemical hardness-softness and polarizability of the molecule and hence its biological activity [48,49].

The energy values of HOMO are computed as -6.089, -5.903 eV and LUMO are -2.845, -2.675 eV, and the energy gap values are 3.244 and 3.227 eV for compound **4a** and **4b**, respectively. Computed values of  $\Delta E_{L-H}$  shows that compound

**4b** is more reactive than compound **4a**. This is also, in accord with the calculated chemical softness 0.308 and 0.310 for compound **4a**, and **4b**, respectively.

HOMO and LUMO plots of compound **4a** and **4b** are presented in Figure 5. As can be seen in Figure 5, the HOMO of compound **4a** is delocalized mainly on the azo nitrogen, carbons that are ortho and para to the azo group, naphthalene ring (except for C3-C4) and O-pyran. C1-C6, C3-C4 and C8-C9 bonds show anti-bonding nature where no electron projection at these regions. LUMO of compound **4a** is being participated mainly from C7 and C9 as well as bonds of C4-C5, C10-N17 and C19-N18. It is clear from Figure 5 that, the LUMO of compound **4a** shows antibonding character over the C-H bonds, *p*-chlorophenyl ring.

The HOMO of compound **4b** is delocalized on bonds of C1-C2, C5-C6, C7-C8, C9-C10, N21-N22, C23-C24 and C23-C25. LUMO of compound **4b** is being participated mainly from C7, C9, C1, C2, and C6 as well as bonds of C4-C5, C10-N17 and C19-N18.

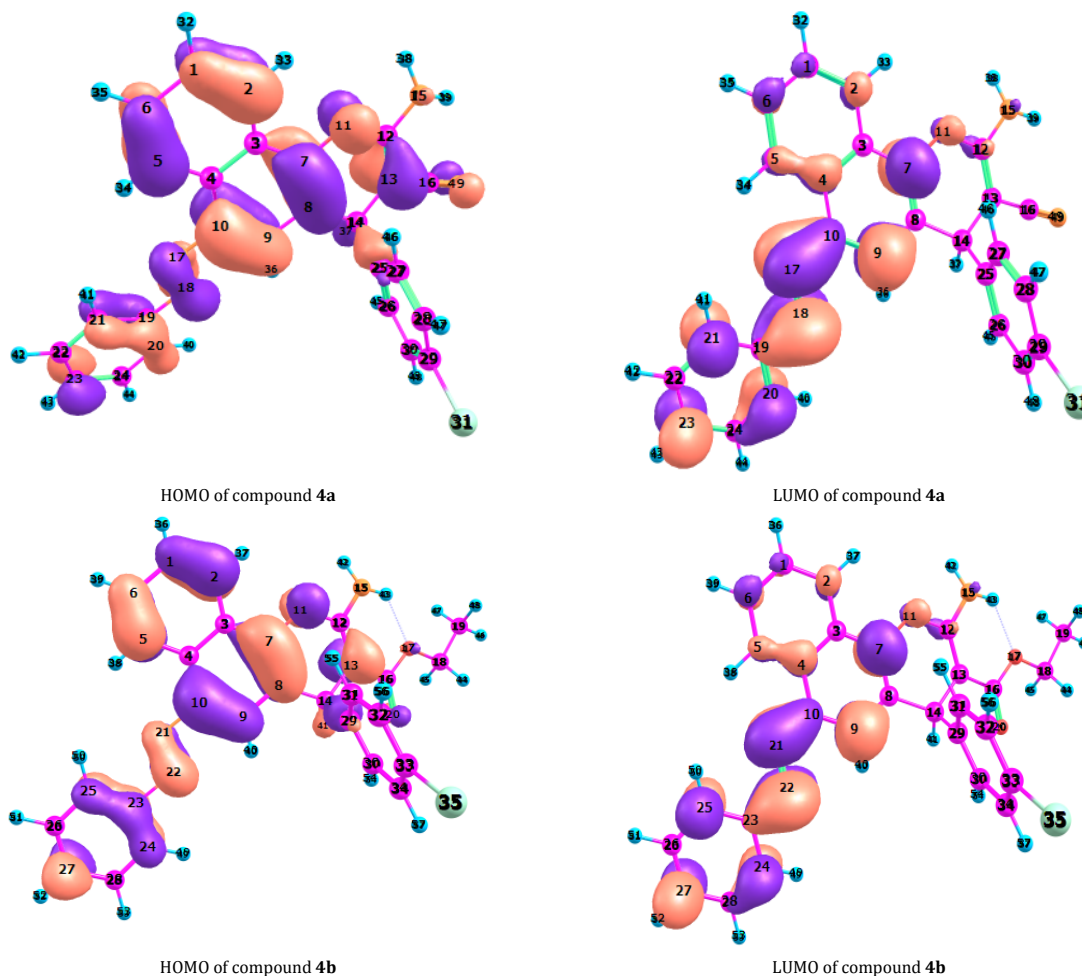


Figure 5. HOMO and LUMO plots of compound 4a and 4b.

#### 4. Conclusion

Efficient one-pot three-component method for the synthesis of various 4*H*-naphthopyran derivatives by reaction of aldehydes, malononitrile or ethyl cyanoacetate cyano ester and 4-phenyldiazonyl-1-naphthol catalyzed by piperidine is reported. The density functional theory was employed to compute molecular geometry of compound **4a** and **4b** at B3LYP/6-31+G(d) level. Amine tautomers are about 7.158 and 8.726 kcal/mole lower energy than imine tautomers for compound **4a** and **4b**, respectively. This difference allows separation at room temperature. Larger energy difference was found for compound **4b** due to extra stabilization produced from intra molecular hydrogen bonding NH...O of distance 1.977 Å. Conformers of the imine molecule are convertible at room temperature as they are less than one kcal/mol. Molecular reactivity descriptors including global electrophilicity, hardness, softness and local condensed Fukui functions were computed. Molecular reactivity descriptors, quantitatively, suggests that compound **4b** is more reactive than compound **4a**.

#### References

- [1]. Wojciechowski, K.; Wyrebak, A.; Gumulak, J. *Dyes Pigments* **2003**, *56*, 99-106.
- [2]. Rudyk, H.; Knaggs, M. H.; Vasiljevic, S.; Hope, J.; Birkett, C.; Gilbert, I. H. *Eur. J. Med. Chem.* **2003**, *38*, 567-579.
- [3]. Mittal, A.; Kurup, L.; Mittal, J. *J. Hazard. Mater.* **2007**, *142*, 243-248.
- [4]. Wainwright, M. *Dyes Pigments* **2008**, *76*, 582-589.
- [5]. Ahmed, A. E. I.; Hay, J. N.; Bushell, M. E.; Wardell, J. N.; Cavalli, G. *React. Funct. Polym.* **2008**, *68*, 248-260.
- [6]. Simu, G.; Chicu, S. A.; Morin, N.; Schmidt, W.; Sisu, E. *Turk. J. Chem.* **2004**, *28*, 579-585.
- [7]. Simu, G. M.; Hora, S. G.; Grad, M. E.; Sisu, E. N. V. *Rev. Roum. Chim.* **2005**, *50*, 113-117.
- [8]. Bae, J. S.; Freeman, H. S.; El-Shafei, A. *Dyes Pigments* **2003**, *57*, 121-129.
- [9]. Combellas, C.; Kanoufi, F.; Pinson, H.; Podyorica, F. *Am. Chem. Soc.* **2008**, *34*, 429-436.
- [10]. Pinson, J.; Podyorica, F. *Chem. Soc. Rev.* **2005**, *34*, 429-444.
- [11]. Dabbagh, H. A.; Teimouri, A.; Chermahini, A. N. *Dyes Pigments* **2007**, *73*, 239-244.
- [12]. Murray, P. S.; Ralph, S. F. *Electrochimica Acta* **2006**, *51*, 2471-2476.
- [13]. Garg, H. G.; Praksh, C. J. *Med. Chem.* **1972**, *15*, 435-436.
- [14]. Browing, C. H.; Cohen, J. B.; Ellingworth, S.; Gulbransen, R. *Journal Storage* **1926**, *100*, 293-25.
- [15]. Khalid, A.; Arshad, M.; Crowley, D. E. *Appl. Microbiol. Biotech.* **2008**, *78*, 361-369.
- [16]. Pagga, U.; Brown, D. *Chemosphere.* **1986**, *15*, 479-491.
- [17]. Farghaly, T. A.; Abdallah, Z. A. *Arkivoc* **2008**, *17*, 295-305.
- [18]. El-Agrody, A. M.; Abd El-Latif, M. S.; El-Hady, N. A.; Fakery, A. H.; Bedair, A. H. *Molecules* **2001**, *6*, 519-527.
- [19]. Bedair, A. H.; El-Hady, N. A.; Abd El-Latif, M. S.; Fakery, A. H.; El-Agrody, A. M. *Il-Farmaco* **2000**, *55*, 708-714.
- [20]. El-Agrody, A. M.; El-Hakim, M. H.; Abd El-Latif, M. S.; Fakery, A. H.; El-Sayed, E. S. M.; El-Ghareab, K. A. *Acta Pharm.* **2000**, *50*, 111-120.
- [21]. Abd El-Wahab A. H. F. *Pharmaceuticals* **2012**, *5*, 745-757.
- [22]. Smith, W. P.; Sollis, L. S.; Howes, D. P.; Cherry, C. P.; Starkey, D. I.; Cobley, N. K. *J. Med. Chem.* **1998**, *41*, 787-797.



- [23]. Taylor, R. N.; Cleasby, A.; Singh, O.; Sharzynski, T.; Wonacott, J. A.; Smith, W. P.; Sollis, L. S.; Howes, D. P.; Cherry, C. P.; Bethell, R.; Colman, P.; Varghese, J. J. *Med. Chem.* **1998**, *41*, 798-807.
- [24]. Hiramoto, K.; Nasuhara, A.; Michiloshi, K.; Kato, T.; Kikugawa, K. *Mutation Res.* **1997**, *395*, 47-56.
- [25]. Martinez, A. G.; Marco, L. J. *Bioorg. Med. Chem. Lett.* **1997**, *7*, 3165-3170.
- [26]. Dell, C. P.; Smith, C. W., European Patent Applications EP 537949, Chem. Abstr. 1993, 119, 139102d.
- [27]. Bianchi, G.; Tava, A. *Agric. Biol. Chem.* **1987**, *51*, 2001-2002.
- [28]. Mohr, S. J.; Chirigos, M. A.; Fuhrman, F. S.; Pryor, J. W. *Cancer Res.* **1975**, *35*, 3750-3754.
- [29]. Al-Ghamdi, A. M.; Abd EL-Wahab, A. H. F.; Mohamed, H. M.; El-Agrody, M. A. *Letts. Drug Des. Discov.* **2012**, *9*, 459-470.
- [30]. Eiden, F.; Denk, F. *Arch. Pharm. Weinheim Ger. (Arch. Pharm.)* **1991**, *324*, 353-354.
- [31]. Frisch, M. J.; Trucks, G. W.; Schlegel, H. B.; Scuseria, G. E.; Robb, M. A.; Cheeseman, J. R.; Montgomery, Jr., J. A.; Vreven, T.; Kudin, K. N.; Burant, J. C.; Millam, J. M.; Iyengar, S. S.; Tomasi, J.; Barone, V.; Mennucci, B.; Cossi, M.; Scalmani, G.; Rega, N.; Petersson, G. A.; Nakatsuji, H.; Hada, M.; Ehara, M.; Toyota, K.; Fukuda, R.; Hasegawa, J.; Ishida, M.; Nakajima, T.; Honda, Y.; Kitao, O.; Nakai, H.; Klene, M.; Li, X.; Knox, J. E.; P. Hratchian, H.; Cross, J. B.; Adamo, C.; Jaramillo, J.; Gomperts, R.; Stratmann, R. E.; Yazyev, O.; Austin, A. J.; Cammi, R.; Pomelli, C.; Ochterski, J. W.; Ayala, P. Y.; Morokuma, K.; Voth, G. A.; Salvador, P.; Dannenberg, J. J.; Zakrzewski, V. G.; Dapprich, S.; Daniels, A. D.; Strain, M. C.; Farkas, O.; Malick, D. K.; Rabuck, A. D.; Raghavachari, K.; Foresman, J. B.; Ortiz, J. V.; Cui, Q.; Baboul, A. G.; Clifford, S.; Cioslowski, J.; Stefanov, B. B.; Liu, G.; Liashenko, A.; Piskorz, P.; Komaromi, I.; Martin, R. L.; Fox, D. J.; Keith, T.; Al-Laham, M. A.; Peng, C. Y.; Nanayakkara, A.; Challacombe, M.; Gill, P. M. W.; Johnson, B.; Chen, W.; Wong, M. W.; Gonzalez, C.; Pople, J. A. et al., Gaussian 09, revision A.02, Gaussian, Inc., Wallingford CT, 2009.
- [32]. Delley B. J. *Chem. Phys.* **1990**, *92(1)*, 508-517.
- [33]. Delley B. J. *Chem. Phys.* **2000**, *113(18)*, 7756-7764.
- [34]. Accelrys Software Inc., Material Studio Modeling Environment, Release v7.0, San Diego: Accelrys Software Inc., 2013.
- [35]. Mostafa, M. K.; Ashraf, H. F. A.; Fathy, A. E.; Ahmed, M. E. *II Farmaco* **2002**, *57*, 715-722.
- [36]. El-Agrody, A. M.; Emam, H. A.; El-Hakim, M. H.; Abd El-Latif, M. S.; Fakery, A. H. J. *Chem. Res. (S)* **1997**, *9*, 320-321.
- [37]. El-Agrody, A. M.; Emam, H. A.; El-Hakim, M. H.; Abd El-Latif, M. S.; Fakery, A. H. J. *Chem. Res. (M)* **1997**, *9*, 2039-2048.
- [38]. Fathy, A. E.; Ashraf, H. F. A.; Gameel, A. M. E.; Mostafa, M. K. *Acta Pharm.* **2004**, *54*, 13-26.
- [39]. Ashraf, H. F. A.; Hany, M. M.; Ahmed, M. E.; Ahmed, H. B. *Eur. J. Chem.* **2013**, *4(4)*, 467-483.
- [40]. Radini, I. A.; El-Wahab, A. H. F. A. *Eur. J. Chem.* **2010**, *7(2)*, 230-237.
- [41]. Wolinsky, J.; Hauer, H. S. *J. Org. Chem.* **1969**, *34*, 3169-3170.
- [42]. Parthasarathi, R.; Padmanabhan, J.; Subramanian, V.; Maiti, B.; Chattaraj, P. K. *J. Phys. Chem. A* **2003**, *107(48)*, 10346-10352.
- [43]. Fukui, K.; Yonezaw, T.; Shingu, H. *J. Chem. Phys.* **1952**, *20*, 722-725.
- [44]. Parr, R. G.; Yang, W. *J. Am. Chem. Soc.* **1984**, *106*, 4049-4050.
- [45]. Yang, W.; Parr, R. G. *Natl. Acad. Sci. U. S. A.* **1985**, *82*, 6723-6726.
- [46]. Gunasekaran, S.; Balaji, R. A.; Kumeresan, S.; Anand, G.; Srinivasan, S. *Can. J. Anal. Sci. Spectrosc.* **2008**, *53*, 149-162.
- [47]. Durig, J. R.; Little, T. S.; Gounev, T. K.; Gardner, J. K.; Sullivan, J. F. *Mol. Struct.* **1996**, *375(1)*, 83-94.
- [48]. Kosar, B.; Albayrak, C. *Spectrochim. Acta. A* **2011**, *78(1)*, 160-167.
- [49]. Sajan, D.; Lakshmi, K. U.; Erdogdu, Y.; Joe, I. H. *Spectrochim. Acta. A* **2011**, *78(1)*, 113-121.